- Synthetic DNA for Cell Surface Engineering:
- 2 Experimental Comparison between Click
- 3 Conjugation and Lipid Insertion in Cell Viability,
- 4 Engineering Efficiency and Displaying Stability
- 5 Xuelin Wang, Connie Wen, Brandon Davis, Peng Shi, Lidya Abune, Kyungsene Lee, Cheng Dong
- 6 and Yong Wang\*
- 7 Department of Biomedical Engineering, The Pennsylvania State University, University Park,
- 8 Pennsylvania 16802, USA
- 9 KEYWORDS: Cell surface engineering, DNA nanotechnology, cell viability, cell assembly,
- 10 tissue engineering.
- ABSTRACT. The cell surface can be engineered with synthetic DNA for various applications
- ranging from cancer immunotherapy to tissue engineering. However, while elegant methods such
- as click conjugation and lipid insertion have been developed to engineer the cell surface with DNA,
- 14 little effort has been made to systematically evaluate and compare these methods. Resultantly, it
- is often challenging to choose a right method for a certain application or to interpret data from
- different studies. In this study, we systematically evaluated click conjugation and lipid insertion in
- cell viability, engineering efficiency and displaying stability. Cells engineered with both methods

can maintain high viability when the concentration of modified DNA is less than 25-50  $\mu$ M. However, lipid insertion is faster and more efficient in displaying DNA on the cell surface than click conjugation. The efficiency of displaying DNA with lipid insertion is 10 to 40 times higher than with click conjugation for a large range of DNA concentration. However, the half-life of physically inserted DNA on the cell surface is 3 to 4 times lower than that of covalently conjugated DNA, which depends on the working temperature. While the half-life of physically inserted DNA molecules on the cell surface is shorter than those clicked onto the cell surface, lipid insertion is more effective than click conjugation in the promotion of cell-cell interactions under two different experimental settings. The data acquired in this work are expected to act as a guideline for choosing an approximate method for engineering the cell surface with synthetic DNA or even other biomolecules.

## 1. INTRODUCTION

Cell surface engineering is promising for various applications such as cancer immunotherapy, tissue engineering, cell delivery and biomolecular sensing.<sup>1-5</sup> It can be achieved by transferring exogenous genetic materials into host cells for protein synthesis and transport to the cell membrane.<sup>6</sup> Protein display on the cell surface can last for a long period as the cells can continuously express exogenous genes. However, this method is associated with safety concerns such as insertional mutagenesis.<sup>7</sup> It is also time-consuming and highly expensive.<sup>8, 9</sup> Thus, great efforts have been recently made in developing non-genetic engineering methods.<sup>10, 11</sup> In particular, synthetic DNA for cell surface engineering has recently received significant attention.<sup>12</sup>

The display of synthetic DNA on the cell surface is different from genetic engineering as it does not require genetic manipulation of host cells or have the problem with insertional mutagenesis. In addition, while gene expression is not involved in this non-genetic engineering method, the display of DNA can be further transformed into the display of other biomolecules such as proteins since DNA can be conjugated with any biomolecules. <sup>13-15</sup> Thus, the display of synthetic DNA on the cell surface is a versatile platform for cell surface engineering.

Numerous methods can be applied to display DNA on the cell surface. As synthetic DNA molecules are displayed on the cell surface in the same ways as natural cell surface components through either covalent or non-covalent bonds, those methods for DNA display can be simply classified into two categories: chemical conjugation and physical incorporation. This classification depends on the final covalent or non-covalent state of DNA molecules. Among chemical conjugation methods, click conjugation has recently attracted significant attention as it uses biorthogonal chemistry. Lipid insertion is the most common physical incorporation

method, relying on non-covalent interactions between the lipid bilayer and lipophilic residues (e.g., cholesterol).<sup>22-24</sup> While both methods have been widely used, little effort has been made to systematically examine the stability of DNA on the cell surface, the efficiency of DNA display, and the viability of cells during and after click conjugation. Moreover, little if any evidence was provided in the literature to make a direct comparison between these methods.

As DNA display is a key factor of determining the functions of engineered cells, this study aimed to collect experimental evidence to understand the effects of the two different methods on DNA display and cellular functions. We conjugated DNA onto the cell surface via copper-free click chemistry in the click conjugation method and engineered the cell surface with a DNA-cholesterol (DNA-Chol) conjugate in the lipid insertion method. Different parameters including concentration, temperature and incubation time were all systematically studied. Cell viability, engineering efficiency, and displaying stability were evaluated for the comparison. To further illustrate the differences between the two methods, we also studied their working efficacy in two applications including the formation of 3-D cell spheroids and the recognition between immune and cancer cells.

#### 2. EXPERIMENTAL SECTION

#### 2.1. Materials

- 69 2.1.1 Chemical reagents
- Oligonucleotides (Table S1) were purchased from Integrated DNA Technologies (Coralville, IA). CellTiter 96® AQueous One Solution Cell Proliferation Assay kit was obtained from Promega

(Madison, WI). Dibenzocyclooctyne (DBCO)-PEG4-NHS ester and N-azidoacetylmannosamine-

73 tetraacylated (Ac<sub>4</sub>ManNAz) were purchased from Click Chemistry Tools (Scottsdale, AZ).

- 74 Dulbecco's phosphate buffered saline (DPBS) was obtained from Thermo-Fisher Scientific
- 75 (Waltham, MA). Carboxyfluorescein succinimidyl ester (CFSE) and CellTrace™ Far Red Cell
- 76 Proliferation Kit were purchased from Invitrogen (Carlsbad, CA).

# 77 2.1.2 Biological reagents

- Bovine serum albumin (BSA), fetal bovine serum (FBS), horse serum (HS), minimum
- 79 essential medium (MEM), Roswell Park Memorial Institute (RPMI) 1640 Medium were obtained
- from Thermo-Fisher Scientific (Waltham, MA). 2-Mercaptoethanol, folic acid, myo-Inositol,
- 81 Annexin V-FITC Apoptosis Detection Kit were obtained from Sigma Aldrich (St. Louis, MO).
- 82 Nature killer (NK) cell and CCRF-CEM (CCRF) were obtained from American Type Culture
- 83 Collection (Manassas, VA). CytoTox 96® Non-Radioactive Cytotoxicity kit was obtained from
- 84 Promega (Madison, WI).

85

92

# 2.2 Preparation of dibenzocyclooctyne-modified DNA (DNA-DBCO)

- DNA-DBCO was synthesized using a previous described method. <sup>15</sup> Briefly, 100 μL of DI-
- 87 NH<sub>2</sub> solution (1 mM) was added to 375 μL of modification buffer (1×PBS, 50 mM NaHCO<sub>3</sub>).
- 88 Following that, 25 μL of DBCO-PEG<sub>4</sub>-NHS ester (DMSO, 30 mM) was added and allowed to
- react for 6 h, this step was repeated twice. The reaction was conducted at 25 °C and 1000 rpm on
- a shaker. Subsequently, the DNA-DBCO was collected and purified using a 3 kDa Amicon Ultra
- 91 Centrifugal Filter.

## 2.3 Cell culture

- NK cells were expanded using the MEM supplemented with 0.2 mM inositol, 0.1 mM 2-
- 94 mercaptoethanol, 0.02 mM folic acid, 12.5% horse serum and 12.5% FBS in cell culture flasks.
- 95 CCRF cells were expanded using RPMI 1640 supplemented with 10% FBS in cell culture flasks.

All cells were cultured in a sterile incubator set to maintain an atmosphere of 37 °C, 5% CO<sub>2</sub> and a 95% RH.

# 2.4 Engineering of the cell surface with DNA molecules using lipid insertion

One million of NK cells were centrifuged into a pellet, and washed twice with DPBS. The resulting cell pellet was dispersed in 500  $\mu$ L MEM, before adding DNA-Chol to pre-determined concentrations (0.25, 0.5, 1, 10, 25 or 50  $\mu$ M). The cells were incubated at 25 °C and 120 rpm on a shaker. After a 30 min incubation, the cells were pelleted and washed with DPBS twice by centrifugation to remove the free DNA-Chol.

# 2.5 Engineering of the cell surface with DNA molecules using click conjugation

NK cells were cultured in proper culture medium supplemented with various concentrations of Ac<sub>4</sub>ManNAz (25, 50, 75 or 100 μM). At predetermined time points (1, 2 or 3 days), cells were collected and washed twice with DPBS. The cells were then dispersed in MEM at a density of 1×10<sup>6</sup> cells/mL and DNA-DBCO was added, followed by incubation at 25 °C and 120 rpm on a shaker. After a 30 min incubation, the cells were then pelleted and washed with DPBS twice by centrifugation to remove the free DNA-DBCO.

#### 2.6 Examination of Cell viability

The CellTiter 96® AQueous One Solution Cell Proliferation Assay kit was used to determine the cell viability of the engineered NK cells. The cells were transferred to a 96-well clear, flat-bottom microplates (Corning Life Sciences) and 20  $\mu$ L CellTiter 96® AQueous One Solution reagent was added to each well. After 3 h incubation, the absorbance was measured using an Infinite M200 Pro microplate reader (Tecan; Grödig, Austria) at 490 nm. All the samples were triplicate (n = 3).

- 118 2.6.1 The cytotoxicity of different Ac<sub>4</sub>ManNAz concentration
- NK cells were seeded in 96-well microplates at a density of  $1 \times 10^4$  cells/well in  $100 \,\mu$ L
- 120 culture medium. Different concentrations of Ac<sub>4</sub>ManNAz (25, 50, 75 or 100 μM) were added into
- the wells. After 2 days, the cell viability was determined. All the samples were triplicate (n = 3).
- 122 2.6.2 The cytotoxicity of Ac<sub>4</sub>ManNAz incubation time
- NK cells were seeded in 96-well microplates at a density of  $1 \times 10^4$  cells/well in  $100 \,\mu$ L
- 124 culture medium. 50 μM Ac<sub>4</sub>ManNAz were then added into the wells. The cell viability was
- assessed after  $Ac_4ManNAz$  treatment for 1, 2, 3 days. All the samples were triplicate (n = 3).
- 126 *2.6.3 The cytotoxicity of different DNA concentration*
- NK cells were dispersed in MEM at a density of  $1 \times 10^6$  cells/mL. Different concentrations
- of DNA (0.25, 0.5, 1, 10, 25 or 50  $\mu$ M) were added. The cells were incubated at 25 °C and 120
- 129 rpm on a shaker. After 30 min incubation, the cells were pelleted and washed with DPBS twice by
- centrifugation to remove the free DNA. The collected cells were seeded into 96-well microplates
- in 100  $\mu$ L MEM and the cell viability was tested. All the samples were triplicate (n = 3).
- 132 2.6.4 The cytotoxicity of different DNA-Chol / DNA-DBCO concentration
- DNA-Chol and DNA-DBCO engineered cells were prepared as described in section 2.4 and
- in section 2.5. The modified cells were seeded into 96-well microplates in 100 µL MEM and the
- cell viability was examined. All the samples were triplicate (n = 3).

# 2.7 Analysis of DNA modification efficiency on cell surface

- DNA-decorated cells were collected and subsequently treated with a 1 µM solution of FAM-
- labeled complementary sequence to DNA (cDNA-FAM) in MEM for 30 min. The cells were
- incubated at 25 °C and 120 rpm on a shaker. The fluorescence intensity displayed on cell surface

- 140 was measured using Guava easyCyte flow cytometer (Hayward, CA). The fluorescence intensity
- was used as an indicator of the modification efficiency. All the samples were triplicate (n = 3).
- 142 2.7.1 The effect of different Ac<sub>4</sub>ManNAz concentration on modification efficiency
- NK cells were cultured using the MEM containing Ac<sub>4</sub>ManNAz (25, 50, 75 or 100 μM) for
- 2 days. The cells were washed twice with DPBS and incubated with 50 μM DNA-DBCO for 30
- min as described in section 2.5. 1 μM cDNA-FAM were then added and the fluorescence intensity
- was measured. All the samples were triplicate (n = 3).
- 147 2.7.2 The effect of different Ac4ManNAz incubation time on modification efficiency
- NK cells were cultured using the MEM containing 50 µM Ac<sub>4</sub>ManNAz and incubated for 1,
- 2, 3 days. The cells were washed twice with DPBS and incubated with 50 μM DNA-DBCO for 30
- min as described in section 2.5. 1 μM cDNA-FAM was then added and the fluorescence intensity
- was measured. All the samples were triplicate (n = 3).
- 152 2.7.3 The change of modification efficiency after Ac<sub>4</sub>ManNAz treatment
- NK cells were cultured using the MEM containing 50 µM Ac<sub>4</sub>ManNAz. After a 2-day
- incubation, the fresh culture medium (without Ac<sub>4</sub>ManNAz) was replaced. After 1, 2 or 3 days,
- the cells were washed twice with DPBS and incubated with 50 µM DNA-DBCO for 30 min as
- described in section 2.5. 1 μM cDNA-FAM was then added and the fluorescence intensity was
- measured. All the samples were triplicate (n = 3).
- 158 2.7.4 The effect of different DNA-Chol or DNA-DBCO concentrations on modification efficiency
- NK cells were incubated with different concentrations of DNA-Chol (0.25, 0.5, 1, 10, 25 or
- 160 50 μM) or DNA-DBCO (0.25, 0.5, 1, 10, 25 or 50 μM) as described in section 2.4 and section 2.5.
- 161 The cells were washed twice and incubated with 1 μM cDNA-FAM. The fluorescence intensity

displayed on cell surface was measured via flow cytometry. The FAM-labeled cells were observed using an Olympus IX73 microscope (Center Valley, PA). All the samples were triplicate (n = 3).

# 2.8 Evaluation of DNA stability on cell surface

To examine the stability of DNA-modified cells, time and temperature studies were performed on DNA-modified cells samples prepared as described in section 2.4 and 2.5. Cells were incubated in MEM and collected at the predetermined time points (0, 2, 4, 6, 8 h). After washing twice with DPBS, each cell sample was treated with 1  $\mu$ M cDNA-FAM for 30 min at 120 rpm on a shaker to label the remaining surface DNA. All the samples were triplicate. Fluorescence intensity was measured via flow cytometry and used as an indicator of the residual DNA molecules on cell surface. This study was repeated at 25 °C and 37 °C. The half-life  $(T_{1/2})$  of DNA on cell surface was calculated using OriginLab software. All the samples were triplicate (n = 3).

# 2.9 Generation of cell spheroids

For lipid insertion, CCRF cells were engineered with 0.25  $\mu$ M DNA-Chol and stained with CFSE (1  $\mu$ M for 5 min), the other group of CCRF cells were engineered with 0.25  $\mu$ M cDNA-Chol and stained with cell trace Far Red (1  $\mu$ M for 10 min). The two groups of modified CCRF cells were mixed together at a 1:1 ratio (final cell density of 1×10<sup>6</sup> cells/mL) and shaken at 50 rpm at 25 °C on a shaker for 45 min. The spheroids were imaged using a fluorescent microscope and the sizes of the spheroids were analyzed using ImageJ software. For click conjugation, the study was performed using 50  $\mu$ M DNA-DBCO or 50  $\mu$ M cDNA-DBCO. All the samples were triplicate (n = 3).

#### 2.10 Examination of CCRF-NK interaction

NK cells were stained with a green dye (CFSE, 1 µM for 5 min), while CCRF cells were stained with a red dye (cell trace Far Red, 1 µM for 10 min). Then supramolecular polyvalent aptamer was generated on the cell surface using lipid insertion or click conjugation according to previous reported method.<sup>25</sup> Briefly, NK cells were treated with either 0.25 µM DNA-Chol as described in section 2.4 or 50 µM DNA-DBCO as described in section 2.5. After DNA decoration, the cells were washed twice with DPBS and subsequently mixed with two DNA monomers (DM1 and DM2-Branch, 1 µM) for 1 h to form the DNA polymer scaffolds. Aptamer sequence (Sgc8cBranch) comprised of an aptamer region for binding CCRF cells (Sgc8) and a cBranch region for hybridization to DM2-Branch on the polymer scaffolds was used to treat the cells for 30 min, the concentration of Sgc8-cBranch was 1 µM. The aptamer-modified NK cells were mixed with CCRF at a 1:1 NK to CCRF ratio (final cell density of 1×10<sup>6</sup> cells/mL) and incubated at 37 °C and 90 rpm on a shaker for 45 min. The formed population of NK-CCRF adhesions was analyzed via flow cytometry at 0, 2, 4 h. In flow cytometry analysis, the data cluster appeared in the upper right quadrant of the scatter-plot represented the population of heterotypic NK-CCRF adhesions. FlowJo software was used to determine the percentage of the population. The enhancement binding efficiency after modification was calculated using Eq.1.

%Enhancement binding efficiency = 
$$\frac{N_{Chol/DBCO} - N_{native}}{N_{native}} \times 100$$
 Eq.1

Where  $N_{Chol}$ ,  $N_{DBCO}$  and  $N_{native}$  indicate the percentage of the population of NK-CCRF adhesions in the lipid insertion (DNA-Chol) group, click conjugation (DNA-DBCO) group and native group, respectively. All the samples were triplicate (n = 3).

#### 2.11 Examination of NK-mediated cytotoxicity

183

184

185

186

187

188

189

190

191

192

193

194

195

196

197

198

200

201

202

203

204

205

To investigate the NK-mediated cytotoxicity to CCRF cells, an apoptosis assay and a lactate dehydrogenase (LDH) assay were conducted. For the apoptosis assay, CCRF cells were seeded

into a 24-well plate at a density of  $1 \times 10^5$  cells/well. NK or aptamer modified-NK cells were co-cultured with CCRF cells at a 1:1 ratio. The cells were collected and the viability of cells was examined by AnnexinV-FITC / propidium iodide (PI) staining. The dot plot was divided into four quadrants (Q1, Q2, Q3, and Q4). Late apoptotic/necrotic, dead cells/debris, early apoptotic and normal cells were localized in the Q1, Q2, Q3 and Q4, respectively. For the LDH assay, CytoTox 96® Non-Radioactive Cytotoxicity kit was used. Briefly, CCRF cells were seeded into a 96-well plate at a density of  $5 \times 10^4$  cells/well. NK or aptamer modified-NK cells were co-incubated with CCRF cells at a 1:1 ratio. The 96-well plate was centrifuged at  $250 \times g$  for 4 min and then incubated in a humidified chamber at  $37^{\circ}$ C with 5% CO<sub>2</sub>. At the different timepoints (4, 12, and 24 h), the 96-well plate was centrifuged at  $250 \times g$  for 4 min. Supernatant (50 µL) was transferred into fresh 96-well plate and 50 µL of CytoTox 96® Reagent solution was added into each well. After the reaction was stopped, the absorbance was measured at 490 nm with a microplate reader. All the samples were triplicate (n = 3).

## 2.12 Statistical Analysis

Prism GraphPad V9.2.0 software was used for statistical analysis. One-way analysis of variance (ANOVA) was performed to compare multiple groups. Student's t-test was performed for the comparison of two groups. A P-value of  $\leq 0.05$  was used to indicate statistical significance.

## 3. RESULTS AND DISCUSSION

# 3.1 Examination of cell viability

An ability to maintain high cell viability is a critical prerequisite for the success of cell surface engineering. Thus, it is necessary to determine how a surface engineering method affects cell viability. To this end, we first examined cell viability after the cell surface was engineered with either click conjugation or lipid insertion (**Figure 1a**).

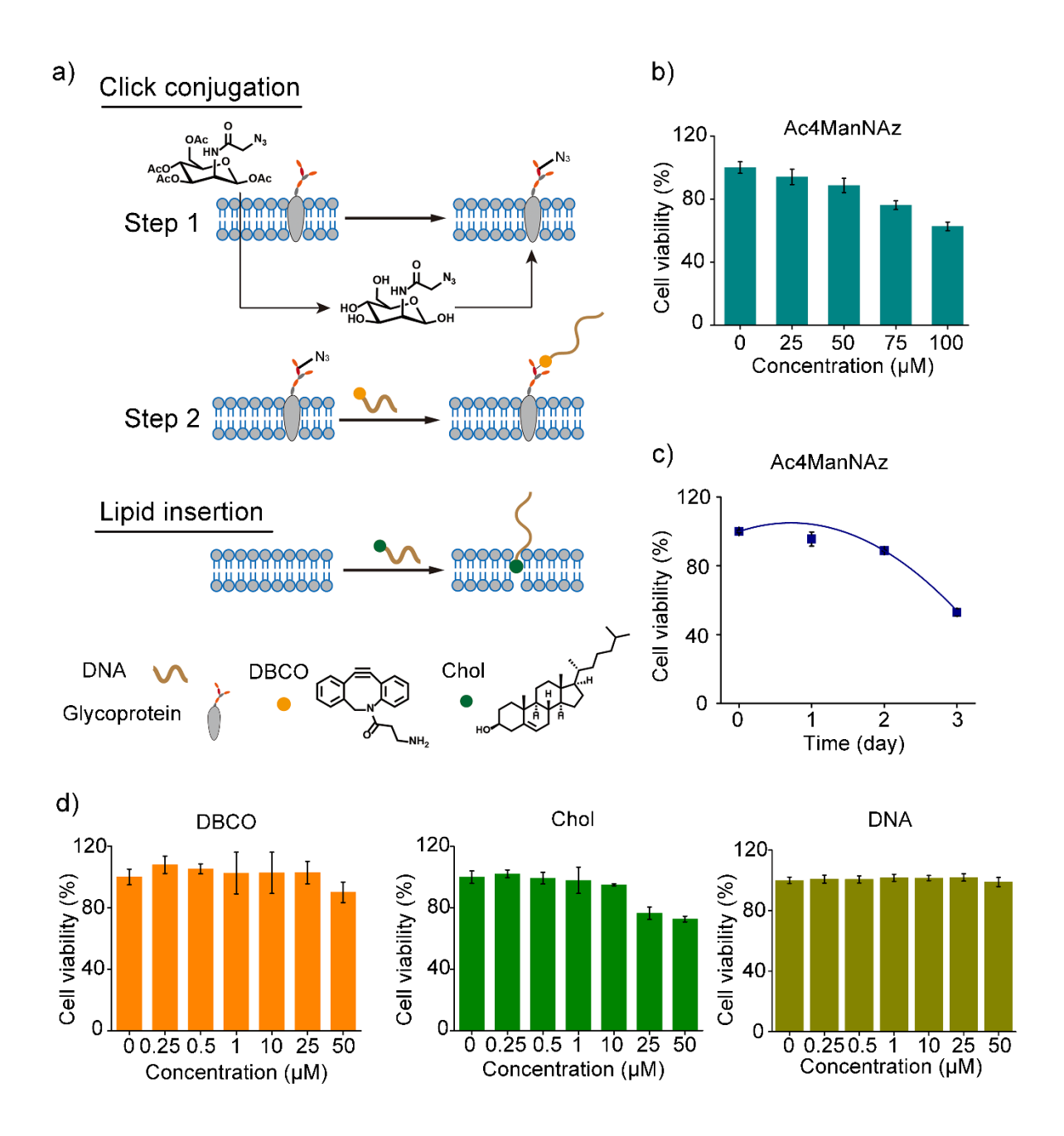


Figure 1. Examination of cell viability. a) Schematic illustration of cell surface engineering with DNA based on click conjugation and lipid insertion. In the click conjugation method, N-azidoacetylmannosamine-tetraacylated (Ac<sub>4</sub>ManNAz) is metabolized and conjugated with glycoproteins for displaying the azide group (N<sub>3</sub>) on the cell surface (step 1). The azide group reacts with dibenzocyclooctyne-modified DNA (DNA-DBCO) to display DNA (step 2). In the lipid insertion method, cholesterol is inserted into the lipid bilayer for DNA display. b) Effect of Ac<sub>4</sub>ManNAz concentration on cell viability. Cells were cultured with Ac<sub>4</sub>ManNAz for two days before the measurement of cell viability. c) Effect of Ac<sub>4</sub>ManNAz treatment time on cell viability. The concentration of Ac<sub>4</sub>ManNAz was 50 μM. d) Effect of DNA-DBCO, DNA-Chol and

unmodified DNA on cell viability. Cells were treated with DNA molecules for 30 min before the measurement of cell viability. DBCO: DNA-DBCO; Chol: DNA-Chol; n = 3 for each group.

239

240

241

242

243

244

245

246

247

248

249

250

251

252

253

254

255

256

257

258

259

260

261

In the click conjugation method, cells were first fed with an azide derivative, i.e., Ac<sub>4</sub>ManNAz. Ac<sub>4</sub>ManNAz is analogues of the natural sialic acid precursor sugar.<sup>26</sup> It can be introduced into the sialic acid biosynthesis pathway resulting in the intracellular conversion into the azide-modified sialic acid analogue. Resultantly, the sialic acid analogue can be displayed on cell surface as a terminal sugar residue of a glycoprotein. <sup>27,28</sup> We then treated the cells with DNA-DBCO for reaction with the azide group on the glycoprotein to display DNA on the cell surface. The cell viability decreased with the concentration of Ac<sub>4</sub>ManNAz. When Ac<sub>4</sub>ManNAz was 100 μM, the cell viability was 63% (Figure 1b). In addition, the cell viability decreased with the incubation time (Figure 1c). The cell viability was decreased to 88% at day 2. However, it further decreased to 53% at day 3. Considering this decrease of cell viability, we treated cells with 50 µM Ac<sub>4</sub>ManNAz for 2 days in the following experiments unless otherwise noticed. After feeding the cells with Ac<sub>4</sub>ManNAz to display the azide group, we incubated the cells with DNA-DBCO and varied its concentration. The cell viability barely changed when the concentration of DNA-DBCO was varied from 0 to 25 µM (Figure 1d). However, when the concentration was further increased to 50 µM, the cell viability started to decrease (Figure 1d).

In the lipid insertion method, Ac<sub>4</sub>ManNAz treatment was not involved. Cells were directly incubated with cholesterol-conjugated DNA (i.e., DNA-Chol) for displaying DNA on the cell surface. When the concentration of DNA-Chol was varied from 0 to 10  $\mu$ M, the cell viability barely changed (**Figure 1d**). However, when the concentration was further increased beyond 10  $\mu$ M, the cell viability decreased significantly. The cell viability decreased to 77% and 73% at 25 and 50  $\mu$ M, respectively.

We observed the decrease of cell viability when both DNA-DBCO and DNA-Chol were used to treat cells. To understand if the decrease of cell viability was caused by DNA or functional groups conjugated to DNA, we treated cells with unmodified DNA (i.e., DNA without either DBCO or Chol). The cell viability barely changed with the concentration of unmodified DNA varied from 0 to 50 µM (Figure 1d). This sharp difference indicates that DNA with modified functional groups can induce cytotoxicity when its concentration reaches a threshold. Under the working conditions presented in this study, the threshold concentrations for DNA-DBCO and DNA-Chol are 50 and 10 µM, respectively. Thus, the data demonstrate that the order of maintaining cell viability is DNA > DNA-DBCO > DNA-Chol. DNA-DBCO exhibits higher biocompatibility than DNA-Chol at a concentration not more than 50 µM. However, in the click conjugation method, Ac<sub>4</sub>ManNAz can cause cytotoxicity prior to cell treatment with DNA-DBCO. Ac<sub>4</sub>ManNAz-induced cytotoxicity is a unique issue to the click conjugation method. Thus, it needs to be balanced to take cell viability into consideration in an application. It is important to note that we used nature killer (NK) cells as a model in this work. Other cells may exhibit a different level of viability in response to Ac<sub>4</sub>ManNAz or DNA treatment.

# 3.2 Examination of engineering efficiency

262

263

264

265

266

267

268

269

270

271

272

273

274

275

276

277

278

279

280

281

282

283

284

Next, we examined the efficiency of engineering the cell surface with DNA. The engineering efficiency was quantified using cDNA-FAM to label DNA displayed on the cell surface (**Figure 2a**). Click conjugation requires the reaction of azide and DBCO. As the azide groups on the cell surface come from intracellular conversion of Ac<sub>4</sub>ManNAz into azide-modified glycoproteins as discussed above, we varied the concentration of Ac<sub>4</sub>ManNAz. The fluorescence intensity virtually doubled when the concentration of Ac<sub>4</sub>ManNAz was increased from 25 to 50 μM (**Figure 2b**). Beyond 50 μM, the fluorescence intensity barely changed. This result suggests that 50 μM was

virtually maximal for NK cells to display the azide groups on their surface. In addition, cells could maintain reasonably high viability at 50  $\mu$ M of Ac<sub>4</sub>ManNAz (**Figure 1b**). Thus, we chose this concentration for other experiments.

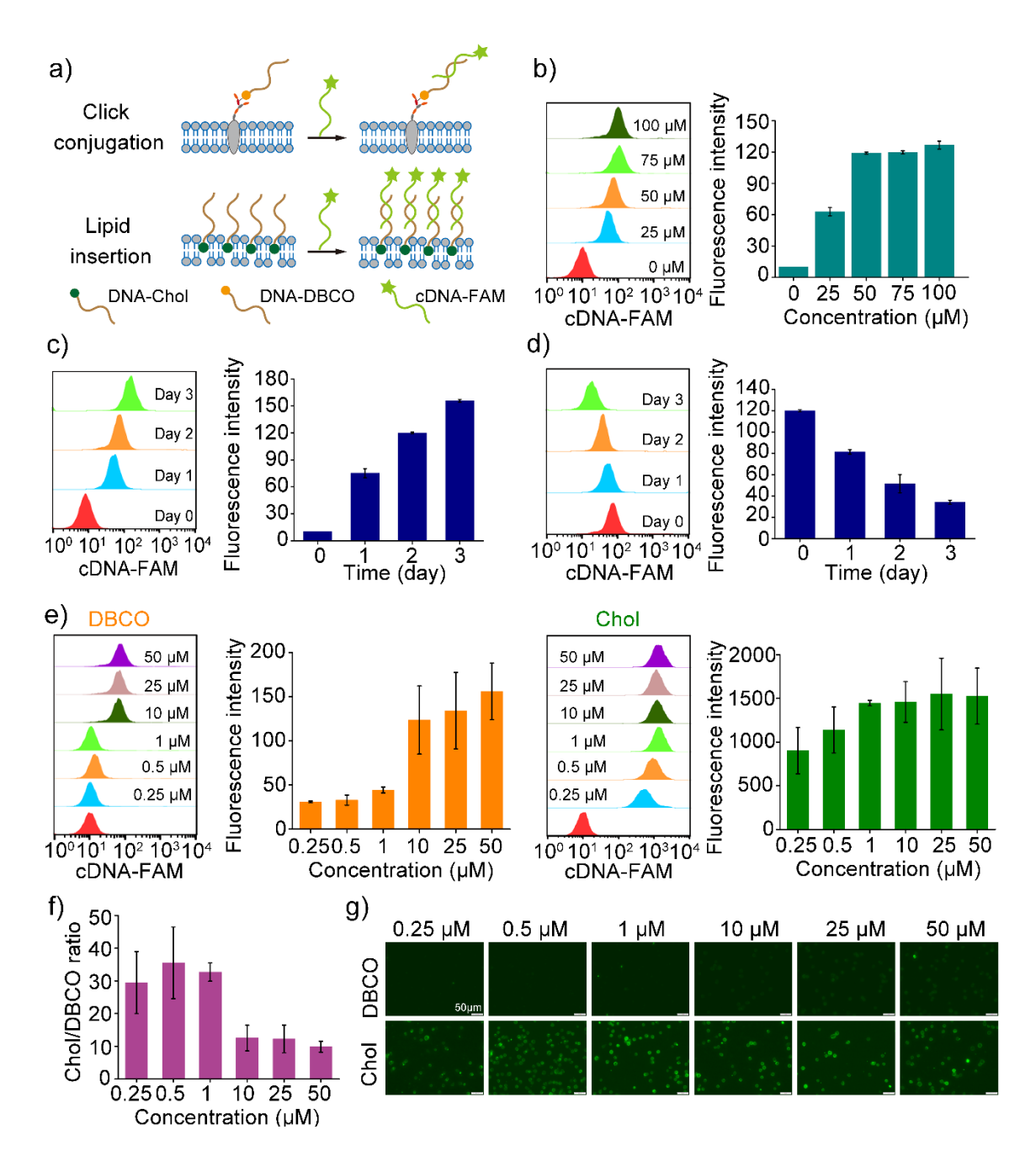


**Figure 2.** Evaluation of surface engineering efficiency. a) Schematic illustration of using cDNA-FAM to label DNA on the cell surface. b) Effect of Ac<sub>4</sub>ManNAz concentration on engineering efficiency. Cells were cultured with Ac<sub>4</sub>ManNAz for two days before reacted with DNA-DBCO. c) Effect of Ac<sub>4</sub>ManNAz treatment time on engineering efficiency. The concentration of

Ac<sub>4</sub>ManNAz was 50  $\mu$ M. d) Effect of cell culture time on engineering efficiency post Ac<sub>4</sub>ManNAz treatment. Cells were treated with 50  $\mu$ M Ac<sub>4</sub>ManNAz treatment for two days and then cultured under normal conditions for three days. Cells were reacted with DNA-DBCO at day 1, 2 and 3 post the two-day Ac<sub>4</sub>ManNAz treatment. e) Effect of DNA-DBCO and DNA-Chol concentrations on engineering efficiency. f) Calculated DNA-DBCO/DNA-Chol ratio in engineering efficiency. g) Representative fluorescence images of cells. Scale bars: 50  $\mu$ m. n = 3 for each group.

293

294

295

296

297298

299

300

301

302

303

304

305

306

307

308

309

310

311

312

313

314

315

316

317

318

We designed two experiments to examine how time affects the engineering efficiency. In the first experiment, the cells were treated with 50 μM Ac<sub>4</sub>ManNAz for three days. At different time points, DNA-DBCO was added to react with the cells (Figure 2c). The data show that the engineering efficiency increased with time, reaching the highest level at day 3 during the 3-day culture. As the level of azide on the cell surface increases with time when the cells were fed with Ac<sub>4</sub>ManNAz continuously, <sup>29</sup> this result indicates that increasing the amount of azide groups on the cell surface led to the increase of DNA conjugation. However, while the data suggest that feeding cells with Ac<sub>4</sub>ManNAz for a longer period is beneficial for improving the engineering efficiency, it is important to balance engineering efficiency and cell viability. Figure 1c shows that cell viability sharply decreased after day 2 and reached 53% at day 3. Thus, feeding NK cells with 50 μM Ac<sub>4</sub>ManNAz for 2 days may be an optimal condition for the click conjugation method. In the second experiment, the cells were treated with 50 µM Ac<sub>4</sub>ManNAz for 2 days. Afterwards, the cell culture medium supplemented with Ac<sub>4</sub>ManNAz was replaced with the normal cell culture medium without Ac<sub>4</sub>ManNAz. The cells reacted with DNA-DBCO at four time points. The engineering efficiency decreased with time (Figure 2d). Our data indicate that the level of azide on the cell surface decreased with time when cells were not treated with Ac<sub>4</sub>ManNAz, suggesting that it is important for cells to react with DNA-DBCO immediately once Ac<sub>4</sub>ManNAz feeding is terminated.

In addition to Ac<sub>4</sub>ManNAz treatment, we studied the effect of DNA-DBCO concentration on the engineering efficiency. When the DNA-DBCO concentration was within the range between 0.25 and 1  $\mu$ M, the fluorescence intensity of cDNA-FAM on the cell surface was extremely low (**Figure 2e**). However, once the DNA-DBCO concentration was increased to 10  $\mu$ M, the fluorescence intensity of cDNA-FAM suddenly increased 3 times (**Figure 2e**). The fluorescence intensity gradually increased with the concentration increased from 10 to 50  $\mu$ M. While the engineering efficiency increased with the DNA-DBCO concentration, it is important to note that a high concentration of DNA-DBCO may cause cytotoxicity (**Figure 1d**).

Next, we studied the efficiency of the lipid insertion method in displaying DNA. To make a fair comparison between lipid insertion and click conjugation, we also varied the DNA-Chol concentrations from 0.25 to 50 μM. DNA-Chol exhibited a significantly different profile of the efficiency versus the concentration when compared to DNA-DBCO. The data show that even at 0.25 μM, DNA-Chol could be effectively displayed on the cell surface (**Figure 2e**). When the concentration of DNA-Chol reached 1 μM, the fluorescence intensity of displayed DNA reached the plateau. In contrast, the fluorescence intensity of displayed DNA was similar to the background when 1 μM DNA-DBCO was used in the click conjugation method. When 0.25 μM DNA-Chol and 50 μM DNA-DBCO were compared, the fluorescence intensity in the former group was almost 6 times higher than the latter. We also calculated the DNA-Chol/DNA-DBCO ratios to make the comparison clearer (**Figure 2f**). The ratios for all tested six concentrations are close to or more than 10. The microscopic imaging is consistent with the flow cytometry analysis (**Figure 2g**).

These data demonstrate that while the cell surface can be efficiently engineered with synthetic DNA using either click conjugation or lipid insertion, lipid insertion is much more efficient than click conjugation. This difference is highly expected as lipids are the major components of the cell membrane and account for 50% of the membrane in weight.<sup>30</sup> The probability for DNA-Chol to be inserted into the lipid bilayer is higher than the conjugation of DNA-DBCO with the azide groups.

Thus, if cell viability and engineering efficiency are the major two factors to consider, we may choose the lipid insertion method. Another advantage of lipid insertion over click conjugation is that lipid insertion does not require additional cell treatment with Ac<sub>4</sub>ManNAz. However, while lipid insertion has these advantages, we also need to consider another important parameter, i.e., displaying stability of DNA on the cell surface.

# 3.3 Examination of displaying stability

Cell membrane is a highly dynamic organelle.<sup>31</sup> For instance, cell receptors continuously recycle between the cell membrane and the cytoplasm.<sup>32, 33</sup> They can also be removed from the cell surface through receptor shedding.<sup>34</sup> When the cell surface is engineered with exogenous biomolecules, their displaying stability needs to be considered. Thus, we further examined the displaying stability of DNA on the cell membrane.

Engineered NK cells were collected at different time points to treat with cDNA-FAM. The FAM intensity was used to indicate the amount and stability of DNA. DNA-Chol exhibited higher fluorescence intensity than DNA-DBCO within the first 2 hours at 37 °C (**Figure 3a**). The opposite result was observed beyond 2 hours. Both DNA-Chol and DNA-DBCO lost intensity quickly. However, their profiles of intensity change are different (**Figure 3b**). The intensity of DNA-DBCO decreased linearly with time whereas the intensity of DNA-Chol decreased exponentially. Based on curve fitting (**Figure 3c**), the t<sub>1/2</sub> of DNA-Chol is 1.6 hours at 37 °C. It is similar to the results reported previously. <sup>16, 35</sup> ENREF 34 In contrast, the t<sub>1/2</sub> of DNA-DBCO is 6 hours. This difference suggests that DNA-DBCO is more stable than DNA-Chol on the cell surface. The short duration of DNA-Chol may be attributed to the internalization of DNA or the dissociation of DNA from the cell surface. Covalently conjugated molecules have been found to remain on the cell surface for 72

hours or even longer.<sup>36</sup> This is reasonable as covalently conjugated molecules will not passively dissociate from the cell surface unless cell receptor shedding is significant.

We also evaluated the displaying stability of DNA at 25 °C to confirm the results obtained at 37 °C. The trends of DNA decrease versus time for both 25 and 37 °C are very similar. It confirms that the amount of DNA-Chol on the cell surface decreased more quickly than that of DNA-DBCO. However, the amount of DNA-Chol was higher than DNA-DBCO at 4 h at 25 °C whereas the former was lower than the latter at 37 °C (**Figure 3d**). We also found that the t<sub>1/2</sub> of DNA-Chol at 25 °C are higher than at 37 °C whereas the t<sub>1/2</sub> of DNA-DBCO virtually maintains the same at two different temperatures (**Figure 3e&f**). These data suggest that a lower temperature is more favorable to enhance the displaying stability of DNA on the cell surface in the lipid insertion method.

# 3.4 Examination of cell-cell interactions after surface engineering

After the basic studies, we used two examples to compare the effectiveness of lipid insertion and click conjugation in promoting cell-cell interactions. The first one is the formation of cell spheroids that hold potential for drug screening or tissue engineering.<sup>37</sup> ENREF 35Cells can naturally form spheroids when suspended in solutions. For instance, the hanging drop technique is a widely used method for the development of cell spheroids.<sup>38</sup> However, such a procedure is slow. In addition, it cannot control or promote cell-cell interaction. New methods have been studied for the generation of cell spheroids.<sup>39</sup> One of them is to use a pair of DNA and cDNA to engineer the cell surface for cell assembly (**Figure 4a**).<sup>21</sup> Thus, we used this application to illustrate the difference between lipid insertion and click conjugation.

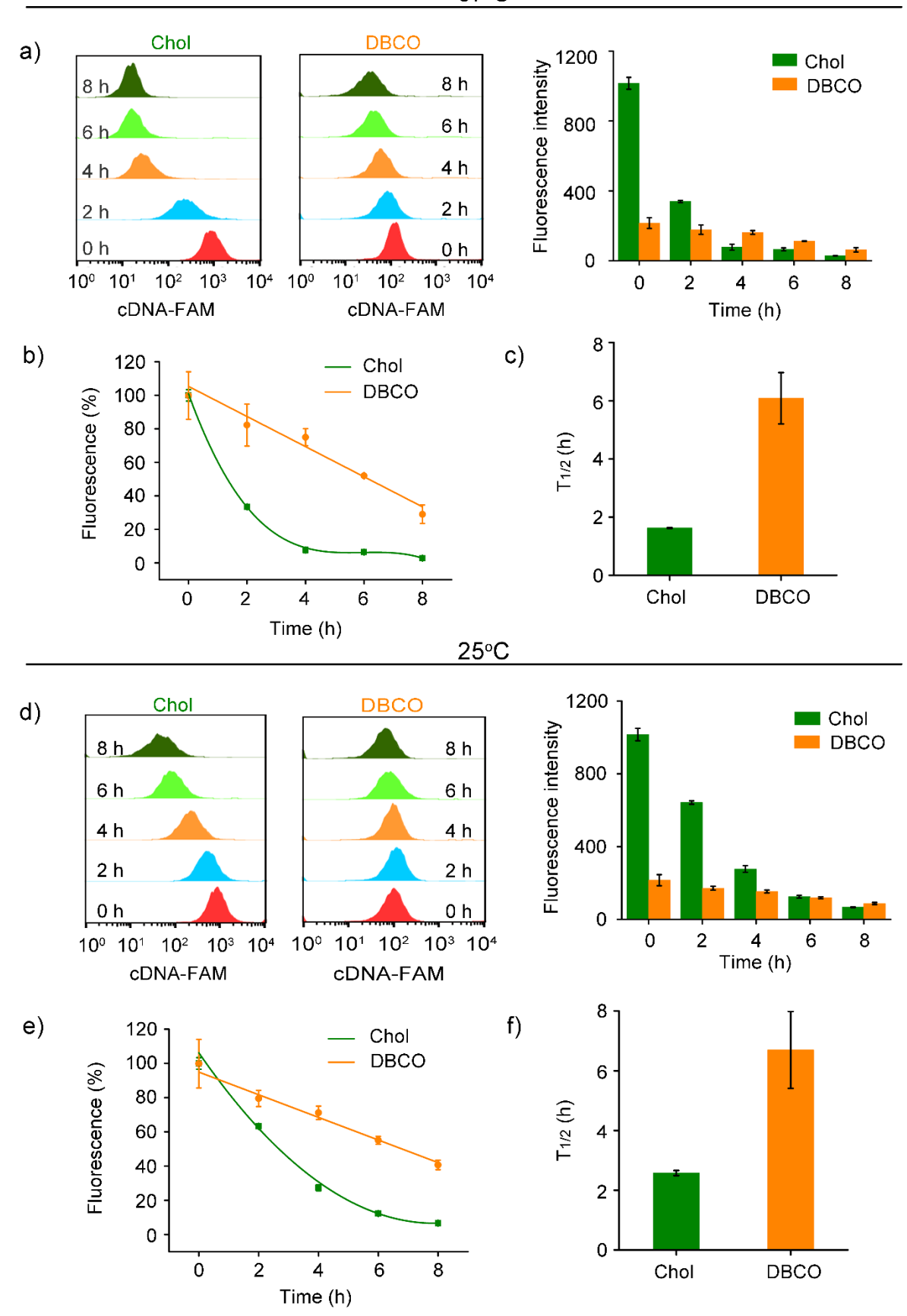


**Figure 3.** Examination of DNA stability on the cell surface at 37 °C (a-c) and 25 °C (d-f), Concentration of DNA-Chol: 0.25 μM; concentration of DNA-DBCO: 50 μM; (n = 3). a,d) Quantification of cell fluorescence using flow cytometry. Engineered cells were analyzed at different time points. b,e) Kinetic analysis of DNA stability on the cell surface. c,f) Comparison of  $t_{1/2}$  values of DNA-Chol and DNA-DBCO. The  $t_{1/2}$  values were acquired according to curve-fitting of the profiles in b and e.

The experimental results show that the average size of spheroids was 128 µm in the DNA-Chol group whereas the size was only 90 µm in the DNA-DBCO group (Figure 4b&c). This difference clearly shows that cells with DNA-Chol are more effective to form larger spheroids than those with DNA-DBCO at the same cell density. This observation is reasonable for two reasons. The cells engineered with DNA-Chol initially had a much higher amount of DNA than those engineered with DNA-DBCO (Figure 3). Moreover, while the data show that DNA-Chol was less stable than DNA-DBCO on the cell surface, cells were used immediately after surface engineering in this application. Thus, the data suggest that DNA stability on the cell surface may not be an important factor for applications such as the formation of DNA spheroids that do not need a long duration of DNA on the cell surface.

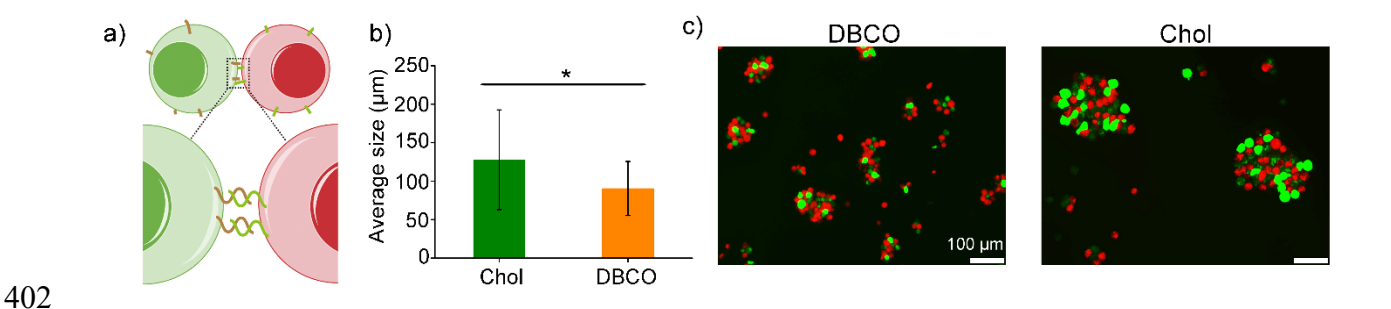


**Figure 4.** Examination of formation of cell spheroids. a) Schematic illustration. b) Average size of cell spheroids. Concentration of DNA-Chol: 0.25  $\mu$ M; concentration of DNA-DBCO: 50  $\mu$ M; (n = 3 for each group). \* p<0.05. c) Representative images of cell spheroids. For clear legibility, engineered cells were separated into two groups that were subsequently labeled with either CFSE (green) or cell trace Far red (red), respectively.

When the cell surface is engineered with single DNA molecules, these molecules can be used as a seed molecule to further develop nanostructures or nanomaterials with new functions. Thus,

in the second example, we engineered the surface of immune cells with a polyvalent aptamer using a method we reported previously and examined the immune-cancer cell interactions (**Figure 5a**).<sup>25</sup> Numerous immune cells have been studied to target cancer cells for cancer immunotherapy.<sup>40,41</sup> A prerequisite for the success of this strategy is strong interactions between the immune and cancer cells.<sup>41,42</sup> We engineered NK cells with the polyvalent aptamer using either lipid insertion or click conjugation. Sgc8 aptamer was used in this experiment. It was selected from DNA library and shown to have high binding affinity and specificity in recognizing CCRF-CEM cells.<sup>43</sup>

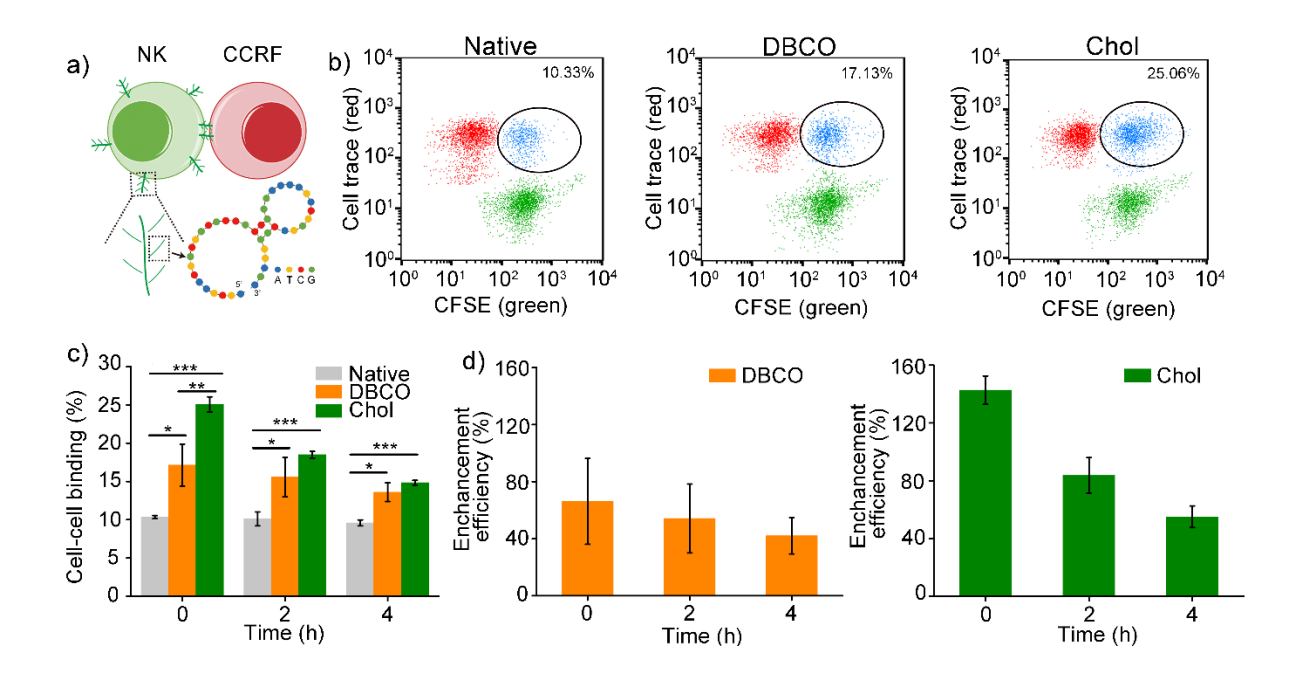


**Figure 5.** Recognition of CCRF-CEM cells by NK cells. a) Schematic illustration of aptamer-mediated cell recognition. b) Representative flow cytometric cytograms showing cell-cell recognition. Concentration of DNA-Chol: 0.25  $\mu$ M; concentration of DNA-DBCO: 50  $\mu$ M. c) Analysis of captured CCRF-CEM cells at different time points, (n = 3), \* p<0.05, \*\* p<0.01, \*\*\* p<0.001. d) Capturing enhancement efficiency of DNA-DBCO and DNA-Chol. Data are presented as mean  $\pm$  standard deviation (n = 3).

Right after the cells were mixed together, the binding percentages of native NK cells, DNA-DBCO engineered NK cells and DNA-Chol engineered NK cells were 10.33%, 17.13%, and 25.06%, respectively (**Figure 5b**). The data show that natural NK cells could bind cancer cells.

This binding capability was significantly increased with NK cells engineered with the polyvalent aptamer. The cells in the DNA-Chol group had a higher binding percentage compared to those in the DNA-DBCO group (**Figure 5b&c**). However, this binding enhancement diminished with time (**Figure 5d**) since the amount of DNA on the cell surface decreased with time (**Figure 3**).

After comparing the ability of NK<sub>native</sub>, NK<sub>DBCO</sub>, NK<sub>Chol</sub> to recognize CCRF-CEM cells, we further studied their ability to kill the cells (**figure S1**). CCRF-CEM cells were stained with AnnexinV-FITC/PI and analyzed using flow cytometry. The data show that the percentages of dead CCRF cells were 25.4% in the NK<sub>native</sub> group, 26.3% in the NK<sub>DBCO</sub> group, 35.4% in the NK<sub>Chol</sub> group, respectively. To confirm the flow cytometry analysis, we also examined cytotoxicity based on LDH release. The NK<sub>Chol</sub> exhibited much higher efficacy in killing CCRF cells than NK<sub>DBCO</sub>.

Based on the above two examples, we compared the effectiveness of lipid insertion and click conjugation in promoting cell-cell interactions. The outcomes of the comparison indicate that lipid insertion may be a better choice for cell surface engineering in comparison to click conjugation under conditions similar to the experimental settings as designed in this work. However, different applications may require different conditions and methods. Thus, we should not simply conclude that lipid insertion is the only choice for the display of DNA on the cell surface in biomedical applications. For example, recently the Cheng group studied *in vivo* click conjugation for targeted drug delivery into tumors. In such a case, click conjugation would be a better choice than lipid insertion that does not have a targeting function. In addition, click conjugation is one of the commonly used chemical conjugation methods. Other methods such as using N-hydroxysuccinimide esters to react with cell surface proteins may lead to the increase of DNA density on the cell surface in comparison to the azide-DBCO click conjugation.

be carried out to further study the efficiency of other methods in displaying DNA in comparison to lipid insertion. Beyond the initial goal of comparing the two methods, the data also suggest that the displaying stability of DNA (or other biomolecules) on the cell surface may need to be further improved if a long duration of DNA display is required.

#### 4. CONCLUSIONS

In this study, we systematically compared click conjugation and lipid insertion in cell viability, engineering efficiency and displaying stability. Both methods have high biocompatibility without causing the significant decrease of cell viability when the concentrations of DNA or sugar substrates are within a certain level. Click conjugation is much less efficient than lipid insertion in displaying DNA on the cell surface. However, chemically conjugated DNA on the cell surface exhibits higher stability. This stability is negatively affected by time and temperature. A significant amount of DNA molecules on the cell surface are lost within several hours for both click conjugation and lipid insertion methods. While the amount of DNA molecules decreases with time on the cell surface, engineered cells exhibit an enhanced capability of cell recognition. Within the experimental setting as designed in this work, lipid insertion is more efficient than click conjugation in displaying DNA for the promotion of cell-cell interactions. Future studies need to be carried out to seek solutions for improving the long-term displaying stability of DNA.

#### ASSOCIATED CONTENT

# **Supporting Information.**

- DNA sequences are listed in the Table S1. The killing efficiency of engineered NK is showed in
- 470 Figure S1.

- 471 AUTHOR INFORMATION
- 472 Corresponding Author
- \*Yong Wang Department of Biomedical Engineering, The Pennsylvania State University,
- 474 University Park, Pennsylvania 16802, USA. Email address: yxw30@psu.edu
- 475 **Author Contributions**
- The manuscript was written through contributions of all authors. All authors have given approval
- 477 to the final version of the manuscript.
- 478 Funding Sources
- This work is in part supported by the U.S. National Science Foundation (1802953), the National
- 480 Institutes of Health (R01HL122311), and American Heart Association (AHA 19IPLOI34770159).
- **481 Notes**
- The authors declare no competing financial interest.
- 483 ACKNOWLEDGMENT
- The authors would like to thank the U.S. National Science Foundation (1802953), the National
- Institutes of Health (R01HL122311), and American Heart Association (AHA 19IPLOI34770159)
- 486 for financial support.
- 487 REFERENCES
- 488 (1) Li, J.; Chen, M.; Liu, Z.; Zhang, L.; Felding, B. H.; Moremen, K. W.; Lauvau, G.; Abadier,
- 489 M.; Ley, K.; Wu, P. A Single-Step Chemoenzymatic Reaction for the Construction of Antibody-
- 490 Cell Conjugates. ACS Cent. Sci. 2018, 4, 1633-1641.

- 491 (2) Teramura, Y.; Iwata, H. Cell Surface Modification with Polymers for Biomedical Studies. *Soft*
- 492 *Matter* **2010**, *6*, 1081-1091.
- 493 (3) Sarkar, D.; Spencer, J. A.; Phillips, J. A.; Zhao, W.; Schafer, S.; Spelke, D. P.; Mortensen, L.
- 494 J.; Ruiz, J. P.; Vemula, P. K.; Sridharan, R.; Kumar, S.; Karnik, R.; Lin, C. P.; Karp, J. M.
- 495 Engineered Cell Homing. *Blood* **2011**, *118*, e184-e191.
- 496 (4) Dosumu, A. N.; Claire, S.; Watson, L. S.; Girio, P. M.; Osborne, S. A. M.; Pikramenou, Z.;
- 497 Hodges, N. J. Quantification by Luminescence Tracking of Red Emissive Gold Nanoparticles in
- 498 Cells. *JACS Au* **2021**, *I*, 174-186.
- 499 (5) Hao, M.; Hou, S.; Li, W.; Li, K.; Xue, L.; Hu, Q.; Zhu, L.; Chen, Y.; Sun, H.; Ju, C.; Zhang,
- 500 C. Combination of Metabolic Intervention and T Cell Therapy Enhances Solid Tumor
- 501 Immunotherapy. Sci. Transl. Med. 2020, 12, eaaz6667.
- 502 (6) Gavins, G. C.; Gröger, K.; Bartoschek, M. D.; Wolf, P.; Beck-Sickinger, A. G.; Bultmann, S.;
- 503 Seitz, O. Live Cell PNA Labelling Enables Erasable Fluorescence Imaging of Membrane Proteins.
- 504 *Nat. Chem.* **2021**, *13*, 15-23.
- 505 (7) Gonçalves, G. A. R.; Paiva, R. M. A. Gene Therapy: Advances, Challenges and Perspectives.
- 506 Einstein, **2017**, 15(3), 369-375.
- 507 (8) Wong, C. H.; Li, D.; Wang, N.; Gruber, J.; Conti, R.; Lo, A. W. Estimating the Financial
- Impact of Gene Therapy in the U.S. NBER Working Papers, 2021, 28628.
- 509 (9) Li, J.; Wang, L.; Tian, J.; Zhou, Z.; Li, J.; Yang, H. Nongenetic Engineering Strategies for
- Regulating Receptor Oligomerization in Living Cells. *Chem. Soc. Rev.* **2020**, *49*, 1545-1568.
- 511 (10) Wang, Q.; Cheng, H.; Peng, H.; Zhou, H.; Li, P. Y.; Langer, R. Non-genetic Engineering of
- 512 Cells for Drug Delivery and Cell-Based Therapy. Adv. Drug Deliver. Rev. 2015, 91, 125-140.

- 513 (11) Csizmar, C. M.; Petersburg, J. R.; Wagner, C. R. Programming Cell-Cell Interactions through
- Non-genetic Membrane Engineering. Cell Chem. Biol. 2018, 25, 931-940.
- 515 (12) Shi, P.; Wang, Y. Synthetic DNA for Cell-Surface Engineering. Angew. Chem., Int. Ed. 2021,
- 516 60, 11580-11591.
- 517 (13) Yang, X.; Li, J.; Pei, H.; Zhao, Y.; Zuo, X.; Fan, C.; Huang, Q. DNA-Gold Nanoparticle
- 518 Conjugates-Based Nanoplasmonic Probe for Specific Differentiation of Cell Types. *Anal. Chem.*
- **2014**, *86*, 3227-3231.
- 520 (14) McMillan, J. R.; Hayes, O. G.; Remis, J. P.; Mirkin, C. A. Programming Protein
- 521 Polymerization with DNA. J. Am. Chem. Soc. 2018, 140, 15950-15956.
- 522 (15) Shi, P.; Zhao, N.; Coyne, J.; Wang, Y. DNA-Templated Synthesis of Biomimetic Cell Wall
- for Nanoencapsulation and Protection of Mammalian Cells. *Nat. Chem.* **2019**, *10*, 2223.
- 524 (16) Borisenko, G. G.; Zaitseva, M. A.; Chuvilin, A. N.; Pozmogova, G. E. DNA Modification of
- Live Cell Surface. *Nucleic Acids Res.* **2009**, *37*, e28-e28.
- 526 (17) Stephan, M. T.; Irvine, D. J. Enhancing Cell Therapies from the Outside in: Cell Surface
- 527 Engineering using Synthetic Nanomaterials. *Nano Today* **2011**, *6*, 309-325.
- 528 (18) Park, J.; Andrade, B.; Seo, Y.; Kim, M.-J.; Zimmerman, S. C.; Kong, H. Engineering the
- 529 Surface of Therapeutic "Living" Cells. *Chem. Rev.* **2018**, *118*, 1664-1690.
- 530 (19) Lamoot, A.; Uvyn, A.; Kasmi, S.; De Geest, B. G. Covalent Cell Surface Conjugation of
- Nanoparticles by a Combination of Metabolic Labeling and Click Chemistry. *Angew. Chem., Int.*
- 532 *Ed.* **2021**, *60*, 6320-6325.
- 533 (20) Shi, P.; Ju, E.; Yan, Z.; Gao, N.; Wang, J.; Hou, J.; Zhang, Y.; Ren, J.; Qu, X. Spatiotemporal
- Control of Cell-Cell Reversible Interactions using Molecular Engineering. *Nat. Commun.* **2016**, 7,
- 535 13088.

- 536 (21) Shi, P.; Zhao, N.; Lai, J.; Coyne, J.; Gaddes, E. R.; Wang, Y. Polyvalent Display of
- 537 Biomolecules on Live Cells. *Angew. Chem., Int. Ed.* **2018**, *57*, 6800-6804.
- 538 (22) Rabuka, D.; Forstner, M. B.; Groves, J. T.; Bertozzi, C. R., Noncovalent Cell Surface
- Engineering: Incorporation of Bioactive Synthetic Glycopolymers into Cellular Membranes. J.
- 540 Am. Chem. Soc. 2008, 130, 5947-5953.
- 541 (23) Ko, I. K.; Kean, T. J.; Dennis, J. E. Targeting Mesenchymal Stem Cells to Activated
- 542 Endothelial Cells. *Biomaterials* **2009**, *30*, 3702-3710.
- 543 (24) Jeong, J. H.; Schmidt, J. J.; Kohman, R. E.; Zill, A. T.; DeVolder, R. J.; Smith, C. E.; Lai,
- M.-H.; Shkumatov, A.; Jensen, T. W.; Schook, L. G.; Zimmerman, S. C.; Kong, H. Leukocyte-
- Mimicking Stem Cell Delivery via in Situ Coating of Cells with a Bioactive Hyperbranched
- 546 Polyglycerol. J. Am. Chem. Soc. 2013, 135, 8770-8773.
- 547 (25) Shi, P.; Wang, X.; Davis, B.; Coyne, J.; Dong, C.; Reynolds, J.; Wang, Y. In Situ Synthesis
- of an Aptamer-Based Polyvalent Antibody Mimic on the Cell Surface for Enhanced Interactions
- between Immune and Cancer Cells. *Angew. Chem., Int. Ed.* **2020**, *59*, 11892-11897.
- 550 (26) Du, J.; Meledeo, M. A.; Wang, Z.; Khanna, H. S.; Paruchuri, V. D. P.; Yarema, K. J.
- Metabolic Glycoengineering: Sialic Acid and Beyond. *Glycobiology* **2009**, *19*, 1382-1401.
- 552 (27) Moons, S. J.; Adema, G. J.; Derks, M. T. G. M.; Boltje, T. J.; Büll, C. Sialic Acid
- Glycoengineering using N-acetylmannosamine and Sialic Acid Analogs. Glycobiology 2019, 29,
- 554 433-445.
- 555 (28) Zhou, X.; Yang, G.; Guan, F. Biological Functions and Analytical Strategies of Sialic Acids
- 556 in Tumor. *Cells* **2020**, *9*, 273.

- 557 (29) Wang, W.; Zhao, Z.; Zhang, Z.; Zhang, C.; Xiao, S.; Ye, X.; Zhang, L.; Xia, Q.; Zhou, D.
- Redirecting Killer T Cells through Incorporation of Azido Sugars for Tethering Ligands.
- 559 *ChemBioChem* **2017**, *18*, 2082-2086.
- 560 (30) Futerman, A. H.; Hannun, Y. A. The Complex Life of Simple Sphingolipids. *EMBO Rep.*
- **2004**, *5*, 777-782.
- 562 (31) Bretscher Mark, S. Membrane Structure: Some General Principles. Science 1973, 181, 622-
- 563 629.
- 564 (32) Maxfield, F. R.; McGraw, T. E. Endocytic Recycling. Nat. Rev. Mol. Cell Bio. 2004, 5, 121-
- 565 132.
- 566 (33) McDonald, F. J. Explosion in the Complexity of Membrane Protein Recycling. *Am. J. Physiol.*
- 567 *Cell Physiol.* **2020**, *320*, C483-C494.
- 568 (34) Montague, S. J.; Andrews, R. K.; Gardiner, E. E. Mechanisms of Receptor Shedding in
- 569 Platelets. *Blood* **2018**, *132*, 2535-2545.
- 570 (35) Palte, M. J.; Raines, R. T. Interaction of Nucleic Acids with the Glycocalyx. J. Am. Chem.
- 571 *Soc.* **2012**, *134*, 6218-6223.
- 572 (36) Tomás, R. M. F.; Gibson, M. I. Optimization and Stability of Cell-Polymer Hybrids Obtained
- 573 by "Clicking" Synthetic Polymers to Metabolically Labeled Cell Surface Glycans.
- 574 *Biomacromolecules* **2019**, *20*, 2726-2736.
- 575 (37) Fang, Y.; Eglen, R. M. Three-Dimensional Cell Cultures in Drug Discovery and
- 576 Development. *SLAS Discov.* **2017**, *22*, 453-455.
- 577 (38) Foty, R. A Simple Hanging Drop Cell Culture Protocol for Generation of 3D Spheroids. J.
- 578 *Vis. Exp.*, **2011**, *51*, e2720.

- 579 (39) Ryu, N.-E.; Lee, S.-H.; Park, H. Spheroid Culture System Methods and Applications for
- 580 Mesenchymal Stem Cells. Cells 2019, 8, 1620.
- 581 (40) Hu, G.; Guo, M.; Xu, J.; Wu, F.; Fan, J.; Huang, Q.; Yang, G.; Lv, Z.; Wang, X.; Jin, Y.
- Nanoparticles Targeting Macrophages as Potential Clinical Therapeutic Agents Against Cancer
- 583 and Inflammation. *Front. Immunol.* **2019**, *10*, 1998.
- 584 (41) Coulie, P. G.; Van den Eynde, B. J.; van der Bruggen, P.; Boon, T. Tumour Antigens
- Recognized by T Lymphocytes: at the Core of Cancer Immunotherapy. Na. Rev. Cancer 2014, 14,
- 586 135-146.
- 587 (42) You, F.; Wang, Y.; Jiang, L.; Zhu, X.; Chen, D.; Yuan, L.; An, G.; Meng, H.; Yang, L. A
- Novel CD7 Chimeric Antigen Receptor-Modified NK-92MI Cell Line Targeting T-cell Acute
- 589 Lymphoblastic Leukemia. Am. J. Cancer Res. 2019, 9, 64-78.
- 590 (43) Xiao, Z.; Shangguan, D.; Cao, Z.; Fang, X.; Tan, W. Cell-Specific Internalization Study of an
- Aptamer from Whole Cell Selection. Chem. -Eur. J. 2008, 14, 1769-1775
- 592 (44) Wang, H.; Wang, R.; Cai, K.; He, H.; Liu, Y.; Yen, J.; Wang, Z.; Xu, M.; Sun, Y.; Zhou, X.;
- Yin, Q.; Tang, L.; Dobrucki, I. T.; Dobrucki, L. W.; Chaney, E. J.; Boppart, S. A.; Fan, T. M.;
- Lezmi, S.; Chen, X.; Yin, L.; Cheng, J. Selective in vivo Metabolic Cell-Labeling-Mediated Cancer
- 595 Targeting. Nat. Chem. Biol. 2017, 13, 415-424.
- 596 (45) Gartner, Z. J.; Bertozzi, C. R. Programmed Assembly of 3-Dimensional Microtissues with
- 597 Defined Cellular Connectivity. *PNAS* **2009**, *106*, 4606-4610.
- 598 (46) Koo, H.; Choi, M.; Kim, E.; Hahn, S. K.; Weissleder, R.; Yun, S. H. Bioorthogonal Click
- 599 Chemistry-Based Synthetic Cell Glue. *Small* **2015**, *11*, 6458-6466.
- 600 (47) Vogel, K.; Glettenberg, M.; Schroeder, H.; Niemeyer, C. M. DNA-Modification of Eukaryotic
- 601 Cells. *Small* **2013**, *9*, 255-262.

# 602 For Table of Contents Only

